

DISCLAIMER

This document was prepared as an account of work sponsored by the United States Government. While this document is believed to contain correct information, neither the United States Government nor any agency thereof, nor the Regents of the University of California, nor any of their employees, makes any warranty, express or implied, or assumes any legal responsibility for the accuracy, completeness, or usefulness of any information, apparatus, product, or process disclosed, or represents that its use would not infringe privately owned rights. Reference herein to any specific commercial product, process, or service by its trade name, trademark, manufacturer, or otherwise, does not necessarily constitute or imply its endorsement, recommendation, or favoring by the United States Government or any agency thereof, or the Regents of the University of California. The views and opinions of authors expressed herein do not necessarily state or reflect those of the United States Government or any agency thereof or the Regents of the University of California.

Compression and Hydration Effects of PFSA Membranes

Ahmet Kusoglu, Adam Z. Weber

Lawrence Berkeley National Laboratory, 1 Cyclotron Rd, MS 70-108B, Berkeley, CA 94720, USA

Abstract

Perfluorosulfonic-acid (PFSA) membranes are still considered to be the benchmark material for proton-exchange-membrane fuel cells. Their performance is controlled by their transport properties and sorption behavior, which are strongly correlated through physiochemical interactions. Furthermore, mechanical properties and membrane stability, which are important for fuel-cell durability, are also governed by the nanomorphology and chemical interactions. Thus, when the membrane is in equilibrium, there exists a balance between the chemical and mechanical properties. Therefore, it is of great interest to understand how this balance is controlled by humidity, temperature, and other external loads. Specifically, it is needed to examine the impact of compression effects on membrane sorption and, hence, transport properties. This paper examines water uptake at both the nanoscale and macroscale showing that compression reduces the water content at both scales, but the effect requires higher pressures than those in typical fuel cells.

Keywords: proton-exchange membrane; sorption; water uptake; compression; fuel cell

1. Introduction

The ionomer membranes used in polymer-electrolyte-fuel-cell (PEFC) applications are always subjected to constraints to some extent due to the cell design and clamping loads to reduce contact resistances (Fig 1). Furthermore, swelling of the membranes due to water

uptake results in compressive stresses during cell operation [1, 2]. However, the effect of the constraints and mechanical loads on the membrane's water uptake behavior is yet to be determined due to the difficulty of such a measurement. Moreover, the lack of the experimental data on the swelling behavior of constrained membranes is a major problem to the understanding of the membrane's response in an operating cell. In this work, we aim to investigate how the constraints on the membrane affect its water uptake behavior and other water-dependent transport properties such as conductivity.

In a fuel cell, to which extent the membranes are constrained depends on a number of factors including, but not limited to, geometry of the cell (e.g. land/channel ratio), thickness and stiffness of the cell components (e.g. bipolar plates, GDL), loads arising during cell operation (swelling) and stack design (e.g. assembly loads due to the clamping of cells). Thus, stresses and pressures in the membrane is not uniform, they are rather dependent on location, time and cell component's material properties. So far, studies focused on the effect of compression on swelling-induced stresses in membranes [2-7], transport in GDL [8-10], and cell resistance and conductivity [11]. Moreover, a number of recent publications on the in-situ neutron imaging of water in fuel cells have provided evidence on the change in the water content of the membrane upon increasing the compression in the cell [12].

Even though a few studies investigating the constraints in fuel cells are available [1, 13, 14], fuel-cell models generally assume that membranes are unconstrained. In fact, there has only been minimal research into swelling of constrained polymers in general with notable exceptions of gels and elastomers, for which Flory-Rehner theory [15, 16] is commonly employed to develop models [17-19]. However, it is debatable that these models, at least in their current form, are applicable to semi-crystalline perfluorinated membranes. Therefore, the water uptake of a compressed/constrained ionomers warrants further investigation, not only theoretically but also experimentally. Weber and Newman [1] studied the effect of constraints

on the water-uptake behavior and conductivity of membranes by means of a macro-homogenous membrane model. Kusoglu et al. [20] developed a mechanics-based model for the swelling pressure in ionomers by accounting for the swelling at microscales. In this work, we extend our previous work [1, 20] on the subject to investigate the equilibrium swelling of ionomer membranes under compression. In the following, first we will briefly explain the origins of constraints in fuel cells followed by the description of swelling equilibrium and the concept of swelling pressure. Then, we will present model predictions for the water content of compressed membranes along with experimental data.

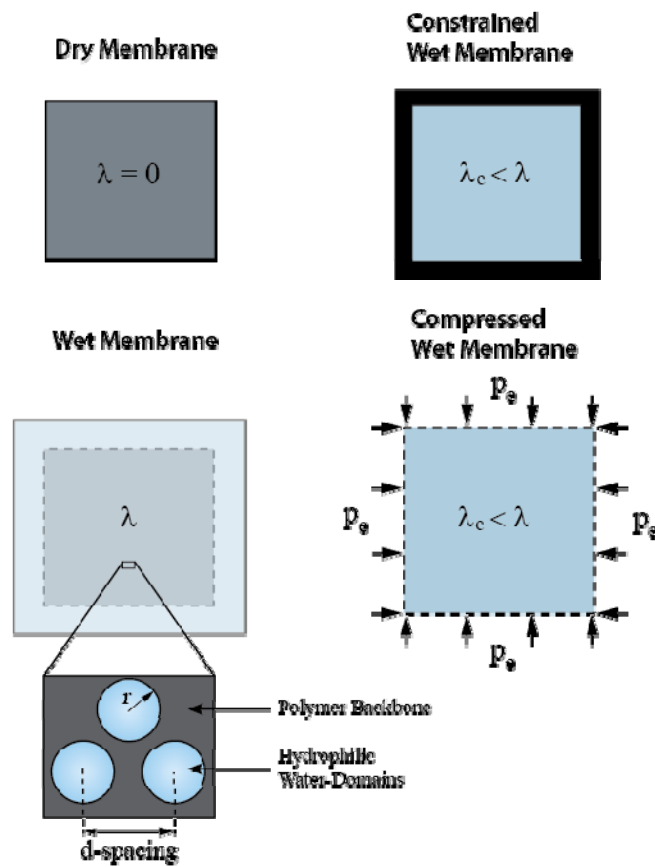


Figure 1. Comparison of a constrained membrane vs. compressed membrane

2. Theory

2.1 Swelling Equilibrium in PFSA membranes

Swelling process of the membrane can be described microscopically as the solvation of ionic groups by the external water in the humid air and then the formation of hydrophilic water-filled domains at nanoscales. Initial water molecules ionize the SO_3^- groups and remain bound to them. Additional water molecules are free to move through the ionomer, causing growth of the clusters and consequently the macroscopic swelling of the membrane. These water domains are separated from the hydrophobic polymer matrix resulting in a two-phase nanostructure [21-31]. As the water uptake increases, these water domains grow, and in some cases coalesce [25, 26, 28, 32-34], causing a continuous structural reorganization in the swollen polymer. However, growth of the water domains deforms the hydrophobic backbone surrounding these domains which drives the osmotic pressure to decrease and therefore limits the swelling [32, 34-39]. Consequently, swelling of a membrane at a given humidity and temperature is governed by the equilibrium of the chemical potentials, which can be written as:

$$\Delta\mu_w^p = \Delta\mu_w^e = RT \ln a_w, \quad (1)$$

$$\Delta\mu_w^p = RT \ln a_p + \bar{V}_w \Pi(p_s)$$

where $\Delta\mu_w^e$ and $\Delta\mu_w^p$ are the chemical potential gradient for the water external and internal to the membrane, respectively, a_w is the activity of the water (or relative humidity), and a_p is the activity of water in the polymer, T is the absolute temperature, R is the universal gas constant, Π is the osmotic pressure, and \bar{V}_w is the molar volume of water ($\bar{V}_w = 18 \text{ cm}^3/\text{mol}$). In equilibrium swelling, the osmotic pressure must be equal to the swelling pressure, P_s , applied by the polymer matrix to the water domains ($\Pi = P_s$). The water activity within the membrane can be expressed using the Flory-Huggins theory for polymer solutions [15]:

$$\ln a_p = \ln(1 - \phi_p) + \left[\left(1 - \frac{1}{\bar{V}_p / \bar{V}_w} \right) \phi_p + \chi \phi_p^2 \right], \quad (2)$$

where χ is Flory–Huggins interaction parameter, which characterizes the enthalpic interactions of mixing between the polymer and solvent, and is ϕ_p is the volume fraction of the polymer including the ionic groups and bound water, i.e. above

$$\phi_p = \frac{\bar{V}_p / \bar{V}_w + \lambda - \lambda^B}{\bar{V}_p / \bar{V}_w + \lambda} \quad (3)$$

where λ^B is the bound water that is strongly attached to ionic groups [35, 40]. The molar volume of the dry polymer, $\bar{V}_p = EW / \rho_p$, is related to the equivalent weight (EW) of the membrane and density, ρ_p . The interaction parameter could be determined empirically from the measured water uptake data for PFSA membranes [35, 41, 42]. As the interaction parameter, χ , for the solvent/polymer decreases, water uptake becomes more favorable and our investigations suggest that the following formula successfully reproduces the experimental data for PFSA membranes:

$$\chi(\phi_p) = 1.9\phi_p^{1.5} \quad (4)$$

2.2 Swelling Pressure

Swelling pressure can be interpreted as the pressure generated in the polymer matrix in response to growing water domains to balance the osmotic pressure. However, it is not easy to describe the swelling pressure due to the complex nature of swelling process in a polymer-water structure that evolves at multiple length scales. One important description is the microscopic swelling, i.e., change in the distance between water domains, *d-spacing*, during water uptake (Fig. 1). The findings of SAXS experiments conducted at different humidities

[22, 23, 25, 26, 28, 32-34, 43, 44] suggest that the plot of macroscopic swelling of the polymer sample vs. d -spacing is linear

$$\frac{d}{d_{\text{dry}}} - 1 = \kappa \left(\frac{L}{L_{\text{dry}}} - 1 \right) = \kappa \left(\phi_p^{-1/3} - 1 \right) \quad (5)$$

where κ is the *non-affine swelling ratio* that characterizes the non-affine nature of the deformation at macro scales (sample length $\sim L$) and smaller scales (domains spacing $\sim d$). Interestingly, the slope was found to be 5 to 5.6, higher than unity [22, 23, 25, 28, 32, 33, 44]. This phenomenon could be attributed to the coalescence of the water domains and/or morphological transitions. Since the swelling pressure is related to the deformation of polymer matrix around the water domains, it is more appropriate to use the d -spacing to characterize swelling pressure. Assuming swelling is a quasi-static process, deformation of the polymer matrix could be modeled by using linear elastic springs connecting the hydrophilic domains throughout the polymer-water network [20]. The springs are assumed to have the temperature-dependent modulus of the polymer backbone E_{pm} [20]. Thus, the pressure generated in the network is due to the radial strain in the deformed backbone during swelling:

$$\frac{p_s}{E_{\text{pm}}} = \frac{\frac{1}{2}d - r}{\frac{1}{2}d_{\text{dry}} - r_{\text{dry}}} = \frac{d}{d_{\text{dry}}} \left(\frac{1 - \phi_{\text{pore}}^{1/n}}{1 - \phi_{\text{pore}}^{\text{dry} 1/n}} \right) \quad (6)$$

where r is the average radius of the hydrophilic water domains (Fig. 1) and n is the dimension of the morphology (e.g. $n = 2$ for a network comprised of cylindrical domains). Eq. (6) suggests that for a highly swollen membrane ($\phi_w \cong 0.25$), the swelling pressure is around 20-25 MPa [20], which is higher than the cell assembly pressures (1-3 MPa), but within the same order of magnitude with the measured values [46-48]. Budinski and Cook [46] developed a compression apparatus to determine the pressure required to reduce the swollen thickness of a

hydrated PFSA membrane back to its initial (dry) value. The PFSA sample was placed in a custom-made cylindrical metal fixture where the membrane is allowed to swell and equilibrate with the water at the bottom side. Then, by applying pressure to the swollen sample using a tight-fit piston and the change in the thickness of the membrane (de-swelling) was measured. Their data are shown in Fig. 22222 along with our model predictions based on the modified swelling pressure as discussed in the next section. As seen from the graph, pressure goes as high as 100 MPa at which up to 80% de-swelling occurs for an initially wet PFSA membrane. Thus, to understand the fundamentals of the effect of compression on swelling, membrane's response and its morphology must be investigated under higher pressures.

2.3 Swelling of a Compressed Membrane

Based on the notion that thermodynamic equilibrium is always maintained independent of the constraint on the membrane [1], swelling of a compressed membrane can be described by modifying the pressure term in the Eq. (1):

$$\Delta\mu_w^p = \Delta\mu_w^{p,c} = RT \ln a_p + \bar{V}_w \Pi(p_s, p_e), \quad (7)$$

The new pressure term becomes a function of the original swelling pressure and the applied external pressure, P_e . Here, we further assumed that water is incompressible. To further simplify the problem, let us focus on the hydrostatic compression. Also, we will assume the applied pressure is the same throughout the polymer-water network. Thus, we can directly add the applied pressure to the original swelling pressure expression (Eq. (6)):

$$\Pi(\phi_w, T) = p_s(\phi_w, T) + p_e \quad (8)$$

Eqs. (7) and (8) solved to determine the water content of an initially hydrated membrane under hydrostatic pressure and the results are plotted in Fig. 2 222 along with the measured

values [46]. As expected, lambda decreases with increasing pressure and the relationship is highly nonlinear. Despite the simplicity of the model and limited experimental data, there is good agreement between the theory and experiments.

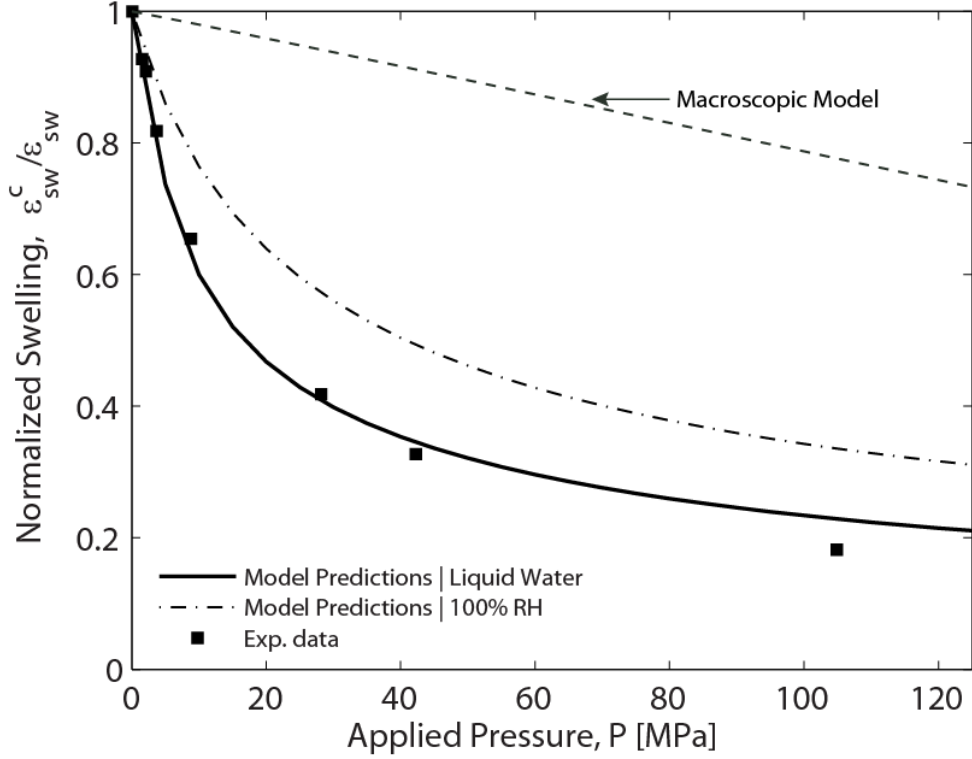


Figure 2. Change in swelling strain as a function of (swelling) pressure at room temperature as predicted from our model compared with the experimental data from ref. [46]. Predictions of a simplified macroscopic model (Eq. (9)) are also included for comparison.

In order to better understand the swelling equilibrium, let's consider a simple macroscopic mechanical model to calculate the water loss under compression without using the chemical potentials and microscopic swelling. Assuming wet membrane undergoes hydrostatic pressure, P_e , de-swelling due to a decrease in the volume (dV) is

$$P_e = -K_b \frac{dV}{V} \quad \text{or} \quad d\varepsilon_{sw}^c = -\frac{dV}{V_{wet}} = \frac{P_e}{K_b(\phi_w)}, \quad (9)$$

where K_b is the effective *bulk modulus* of the swollen-membrane, calculation of which can be found in [49] based on theory in ref. [50]. An interesting aspect of Eq. (9) is that since the bulk modulus of the water (2.2 GPa) is higher than that of a dry membrane (~ 1 GPa [49]), water domains act as filler and therefore increase the bulk modulus of the swollen membrane. It follows from the Fig. 2 that the macro-model underestimates the water loss (de-swelling) under external pressure. Thus it is important to implement the swelling-deformation at micro-scales into thermodynamics equilibrium using. Once we obtain information on the effect of compression -in addition to humidity- on the domain spacing (e.g. $d_s = f(p_e)$) we can easily modify the formulations to have more accurate representation of nano-structural changes during swelling; this is our on-going work.

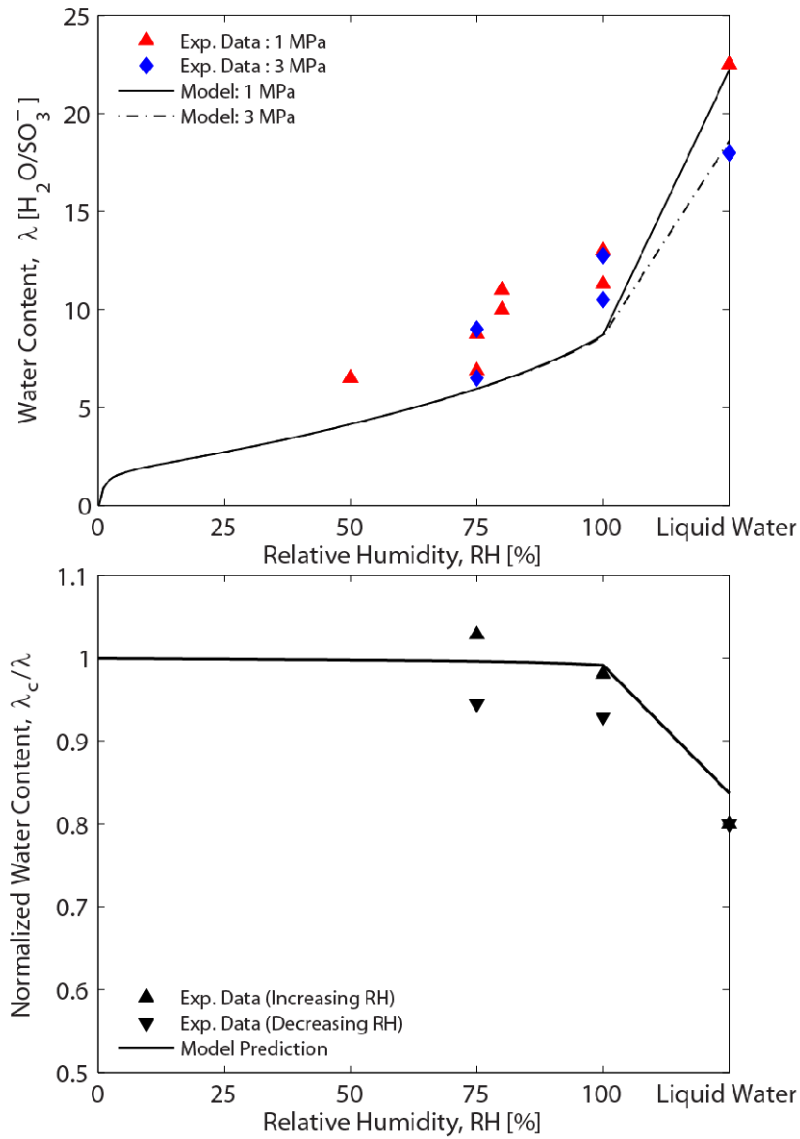


Figure 3 Water uptake of a compressed membrane determined from neutron imaging of a fuel cell setup compared with model predictions: (a) sorption isotherm and (b) normalized water content.

3. Water content of a compressed membrane in a fuel cell setup

The challenges associated with measuring the change in water content of a thin, soft polymer film under compression requires a testing system that is more sophisticated than the

conventional methods (such as weight balance or vapor sorption apparatus). For this purpose, neutron imaging is a powerful method to visualize the water content of the membrane in an operating fuel cell (in-situ) [51-53]. The membrane's water content was found to be dependent on the level of compression in the fuel cell (e.g. clamping force, GDL type/thickness [12]). Researchers at Los Alamos National Laboratory determined the water content of a membrane for various compression pressures. A particular set of data is shown in Fig. 3. In order to explicitly see the compression effect, we normalize the water content of the compressed membrane (3 MPa), λ_c , with that of an uncompressed membrane and plotted λ_c / λ as a function of humidity (Fig 3B). The model predictions agree well with the data suggesting a decrease in water content especially when the membrane is liquid-equilibrated and also that the modeling methodology is appropriate. At low humidities, however, the compression effect is negligible for the pressures investigated.

4. Conclusion

In this paper, we investigated the effect of compression on the water-uptake behavior of proton-exchange membranes. The results suggest that constraining and/or compressing the membrane might reduce its average water content, especially at high humidities and in liquid water. Thus, the mechanical loads acting on the membrane and their effects on the membrane's performance water must be considered in fuel cell models. The experimental data were used to validate the theory in which deformation of the polymer matrix due to the growth of water domains and compression is implemented into the pressure term in thermodynamic equilibrium. Model predictions for the sorption isotherms and swelling strain as a function of external pressure are in good agreement with the measured data.

Acknowledgements

We would like to thank Drs. Rod Borup and Dusan Spornjak of Los Alamos National Laboratory for providing the neutron imaging data. We would also like to thank Drs. Craig Gittleman and Yeh-hung Lai of General Motors for discussion of the Budinski paper and results. This work was funded by the Assistant Secretary for Energy Efficiency and Renewable Energy, Office of Fuel Cell Technologies, of the U. S. Department of Energy under contract number DE-AC02-05CH11231.

References

- 1 A.Z. Weber, J. Newman, *AIChE Journal*, 50 (2004).
- 2 A. Kusoglu, A.M. Karlsson, M.H. Santare, S. Cleghorn, W.B. Johnson, *Journal of Power Sources*, 161 (2006).
- 3 A. Kusoglu, A.M. Karlsson, M.H. Santare, S. Cleghorn, W.B. Johnson, *Journal of Power Sources*, 170 (2007).
- 4 A. Kusoglu, A. Karlsson, M. Santare, S. Cleghorn, W.B. Johnson, *ECS Transactions*, 16 (2008).
- 5 D. Bograchev, M. Gueguen, J.C. Grandidier, S. Martemianov, *Journal of Power Sources*, 180 (2008).
- 6 R. Solasi, Y. Zou, X. Huang, K. Reifsnider, D. Condit, *Journal of Power Sources*, 167 (2007).
- 7 Y.-H. Lai, K.M. Cortney, S.G. Craig, A.D. David, *Journal of Fuel Cell Science and Technology*, 6 (2009).
- 8 S. Escribano, J.F. Blachot, M. Etheve, A. Morin, R. Mosdale, *Journal of Power Sources*, 156 (2006).
- 9 W.R. Chang, J.J. Hwang, F.B. Weng, S.H. Chan, *J. Power Sources*, 166 (2007).
- 10 A. Bazylak, D. Sinton, Z.S. Liu, N. Djilali, *J. Power Sources*, 163 (2007).
- 11 R. Jiang, C.K. Mittelsteadt, C.S. Gittleman, *Journal of the Electrochemical Society*, 156 (2009).
- 12 D. Spornjak, P.P. Mukherjee, R. Mukundan, J. Davey, D.S. Hussey, D. Jacobson, R.L. Borup, *ECS Transactions*, 33 (2010).
- 13 I. Nazarov, K. Promislow, *Journal of the Electrochemical Society*, 154 (2007).
- 14 A. Kusoglu, M.H. Santare, A.M. Karlsson, S. Cleghorn, W.B. Johnson, *Journal of the Electrochemical Society*, 157 (2010).

- 15 P.J. Flory, Principles of polymer chemistry, Cornell University Press, Ithaca, 1953.
- 16 F. Horkay, B. McKenna, Polymer networks and gels, in: J.E. Mark (Ed.) Physical Properties of Polymers Handbook, Springer, New York, 2007, pp. 497-523.
- 17 W. Hong, Z.S. Liu, Z.G. Suo, International Journal of Solids and Structures, 46 (2009).
- 18 R. Marcombe, S.Q. Cai, W. Hong, X.H. Zhao, Y. Lapusta, Z.G. Suo, Soft Matter, 6 (2010).
- 19 X.M. Li, Z. Shen, T. He, M. Wessling, Journal of Polymer Science Part B-Polymer Physics, 46 (2008).
- 20 A. Kusoglu, M.H. Santare, A.M. Karlsson, Polymer, 50 (2009).
- 21 W.Y. Hsu, T.D. Gierke, J. Membr. Sci., 13 (1983).
- 22 M.H. Kim, C.J. Glinka, S.A. Grot, W.G. Grot, Macromolecules, 39 (2006).
- 23 M. Fujimura, T. Hashimoto, H. Kawai, Macromolecules, 15 (1982).
- 24 F.P. Orfino, S. Holdcroft, J. New Mater. Electrochem. Syst., 3 (2000).
- 25 G. Gebel, J. Lambard, Macromolecules, 30 (1997).
- 26 P.J. James, J.A. Elliott, T.J. McMaster, J.M. Newton, A.M.S. Elliott, S. Hanna, M.J. Miles, Journal of Materials Science, 35 (2000).
- 27 A. Gruger, A. Regis, T. Schmatko, P. Colomban, Vibrational Spectroscopy, 26 (2001).
- 28 B. Dreyfus, G. Gebel, P. Aldebert, M. Pineri, M. Escoubes, M. Thomas, Journal De Physique, 51 (1990).
- 29 E.J. Roche, M. Pineri, R. Duplessix, Journal of Polymer Science Part B-Polymer Physics, 20 (1982).
- 30 H.G. Haubold, T. Vad, H. Jungbluth, P. Hiller, Electrochimica Acta, 46 (2001).
- 31 M. Laporta, M. Pegoraro, L. Zanderighi, Physical Chemistry Chemical Physics, 1 (1999).
- 32 G. Gebel, Polymer, 41 (2000).
- 33 T.D. Gierke, G.E. Munn, F.C. Wilson, Journal of Polymer Science, Polymer Physics Edition, 19 (1981).
- 34 W.Y. Hsu, T.D. Gierke, Macromolecules, 15 (1982).
- 35 P. Choi, N.H. Jalani, R. Datta, J. Electrochem. Soc., 152 (2005).
- 36 K.A. Mauritz, C.E. Rogers, Macromolecules, 18 (1985).

- 37 A.Z. Weber, J. Newman, *Journal of the Electrochemical Society*, 151 (2004).
- 38 B. Dreyfus, *J. Polym. Sci., Part B: Polym. Phys.*, 21 (1983).
- 39 A. Eisenberg, *Macromolecules*, 3 (1970).
- 40 H. Takata, N. Mizuno, M. Nishikawa, S. Fukada, M. Yoshitake, *International Journal of Hydrogen Energy*, 32 (2007).
- 41 P. Futerko, I.M. Hsing, *J. Electrochem. Soc.*, 146 (1999).
- 42 R.S. Yeo, *Polymer*, 21 (1980).
- 43 Y. Termonia, *Polymer*, 48 (2007).
- 44 L. Rubatat, A.L. Rollet, G. Gebel, O. Diat, *Macromolecules*, 35 (2002).
- 45 K. Schmidt-Rohr, Q. Chen, *Nature Materials*, 7 (2008).
- 46 M.K. Budinski, A. Cook, *Tsinghua Science & Technology*, 15 (2010).
- 47 M. Escoubes, M. Pineri, E. Robens, *Thermochim. Acta*, 82 (1984).
- 48 K.K. Pushpa, D. Nandan, R.M. Iyer, *J Chem Soc Farad T 1*, 84 (1988).
- 49 A. Kusoglu, M.H. Santare, A.M. Karlsson, S. Cleghorn, W.B. Johnson, *Journal of Polymer Science Part B: Polymer Physics*, 46 (2008).
- 50 Y. Benveniste, *Mechanics Research Communications*, 13 (1986).
- 51 R. Mukundan, R.L. Borup, *Fuel Cells*, 9 (2009).
- 52 R. Mukundan, J.R. Davey, T. Rockward, J.S. Spendelow, B. Pivovar, D.S. Hussey, D.L. Jacobson, M. Arif, R. Borup, *ECS Transactions*, 11 (2007).
- 53 J. Spendelow, R. Mukundan, J. Davey, T. Rockward, D.S. Hussey, D. Jacobson, M. Arif, R.L. Borup, *ECS Transactions*, 16 (2008).